



## Article

# Preparation of Lambda-Cyhalothrin-Loaded Chitosan Nanoparticles and Their Bioactivity against *Drosophila suzukii*

Rady Shawer <sup>1,\*</sup> , Eman S. El-Leithy <sup>2,3</sup>, Rania S. Abdel-Rashid <sup>3</sup>, Abdelazeem S. Eltaweil <sup>4</sup> , Rowida S. Baeshen <sup>5</sup> and Nicola Mori <sup>6</sup>

<sup>1</sup> Department of Plant Protection, Faculty of Agriculture (Saba Basha), Alexandria University, Alexandria 21531, Egypt

<sup>2</sup> Department of Pharmaceutics and Industrial Pharmacy, Faculty of Pharmacy, October University for Modern Sciences and Arts (MSA), Cairo 12451, Egypt

<sup>3</sup> Department of Pharmaceutics and Industrial Pharmacy, Faculty of Pharmacy, Helwan University, Cairo 11795, Egypt

<sup>4</sup> Department of Chemistry, Faculty of Sciences, Alexandria University, Alexandria 21526, Egypt

<sup>5</sup> Department of Biology, Faculty of Science, Tabuk University, Tabuk 71421, Saudi Arabia

<sup>6</sup> Department of Biotechnology, Verona University, 37134 Verona, Italy

\* Correspondence: rady.shawer@alexu.edu.eg; Tel.: +20-1002322033

**Abstract:** The encapsulation of pesticides within nanoparticles is a promising approach of advanced technology in sustainable agriculture. Lambda-cyhalothrin (LC) was encapsulated by the ionotropic gelation technique into chitosan (CS)/tripolyphosphate (TPP) and CS/alginate (ALG) matrixes. CS-LC nanoparticles were characterized, and their efficacy was then evaluated against the key pest of soft fruits in Europe and the United States, *Drosophila suzukii*. The encapsulation efficiency (74%), nanoparticle yield (80%), polydispersity index (0.341), zeta potential (−23.1 mV) and particle size (278 nm) were determined at the optimum conditions. FTIR confirmed the cross-linkage between CS and TPP/ALG in the nanoparticles. The optimum formula recommended by the fractional factorial design was associated with the formulation variables of CS of high or low molecular weight, cross-linking agent (TPP), LC concentration (1.5% *w/v*) and stirring rate (1500 rpm), showing the highest desirability value (0.5511). CS-LC nanoparticles of the lowest particle size (278 nm) exhibited the highest percent mortality of *D. suzukii* males (86%) and females (84%), exceeding that caused by the commercial product (Karate-zeon<sup>®</sup> 10% CS) at 2 HAT. This is the first work to use the ionic gelation technique to make LC nanoparticles, to the best of our knowledge. The encapsulation of chemical pesticides within biodegradable polymeric nanoparticles could be helpful for establishing a sustainable IPM strategy with benefits for human and environmental health and the lifetime of pesticides.

**Keywords:** ionotropic gelation; pyrethroids; tripolyphosphate; alginate; spotted wing drosophila



**Citation:** Shawer, R.; El-Leithy, E.S.; Abdel-Rashid, R.S.; Eltaweil, A.S.; Baeshen, R.S.; Mori, N. Preparation of Lambda-Cyhalothrin-Loaded Chitosan Nanoparticles and Their Bioactivity against *Drosophila suzukii*. *Nanomaterials* **2022**, *12*, 3110. <https://doi.org/10.3390/nano12183110>

Academic Editor: Alexey Pestryakov

Received: 20 July 2022

Accepted: 1 September 2022

Published: 8 September 2022

**Publisher's Note:** MDPI stays neutral with regard to jurisdictional claims in published maps and institutional affiliations.



**Copyright:** © 2022 by the authors. Licensee MDPI, Basel, Switzerland. This article is an open access article distributed under the terms and conditions of the Creative Commons Attribution (CC BY) license (<https://creativecommons.org/licenses/by/4.0/>).

## 1. Introduction

Agricultural production is hampered by a large number of variable insect pests, which cause losses of about 18–20% of annual crop production worldwide, valued at more than USD 470 billion [1]. At present, chemical control is still the main control method used for managing these damaging pests [2–7]. However, the increased use of chemical pesticides on agricultural crops has raised a great number of economic, ecological and health concerns, leading to the development of pest resistance, the elimination of pests' natural enemies—as well as other beneficial species—and environmental pollution [8–14].

Pyrethroids are synthesized as derivatives of the botanical pyrethrin [15,16]. More than 520 tons of pyrethroids are used annually in the pest control worldwide [17]. They have become the main chemical class used in agricultural, veterinary and household pest management [18]. Moreover, they play a vital role in public health. Pyrethroids are most

commonly used for mosquito net control due to their rapid effect at low application rates and their relative safety for human contact and household usage [19,20]. However, their continuous application has caused adverse effects on the environment, human health and beneficial microorganisms [15]. They can cause changes in the plasma biochemical profile and increase SGPT activity in humans [15]. Lambda-cyhalothrin (LC) is one of the most common pyrethroids used for agricultural and household pest control [19,20]. It is a wide-spectrum pyrethroid [21], acting through contact and stomach action on the nervous system [22]. However, LC is a very poorly water-soluble insecticide (5 µg/L at 21 °C) [23].

Given this limited water solubility [24], nanotechnology may offer effective solutions to overcome such drawbacks [25]. Producing nano-formulations able to decrease hazards to the end user and at the same time be efficient in pest control has captured the imagination of researchers, manufacturers and even the general population [26]. Recently, delivery systems have emerged as a promising option for pesticide delivery [26–28]. Chitosan (CS), a synthetic polymer, is one of the most promising polymers used for efficient delivery of agrochemicals because of its proven biocompatibility, biodegradability, non-toxicity and adsorption properties [29,30]. Agrochemicals encapsulated in CS matrices have the ability to function as a protective reservoir for the active ingredients [29]. They showed major advantages over traditional methods, including facilitating the uptake of active ingredients through the cell membrane, protecting ingredients from the surrounding environment and controlling pesticides' release [29].

The ionotropic gelation technique is the most important technique for ionic cross-linking of CS with low molecular weight, hydrophobic and high molecular weight ions [31,32]. It is an electrostatic interaction between differently charged products, one of which at least is a polymer, under mechanical stirring [33,34]. The most commonly used cross-linking agents in this technique are sodium tripolyphosphate (TPP) and alginate (ALG) [33–35]. However, there is still a wide knowledge gap regarding its potential application in the encapsulation of active ingredients of pesticides in agriculture [29].

The present study aimed to prepare CS nanoparticles loaded with LC by the ionotropic gelation technique and to evaluate the bioactivity of the prepared CS-LC nanoparticles against a newly emerged destructive insect, the cherry fly, *Drosophila suzukii* Matsumura (Diptera: *Drosophilidae*), commonly known as the spotted wing drosophila (SWD). It is a highly polyphagous invasive pest, native to Asia, which has recently caused significant damage to a wide variety of berry and stone fruit crops in the United States [36–38], South America [39], Canada [40] and Europe [41,42]. The SWD's polyphagia, the infestation during the ripening stage close to harvest, the length and scale of the harvesting period and the presence of different varieties of its host vary greatly, complicating its chemical control [43]. An adulticide–ovicide and residual approach is needed because effective control of larvae is not possible [6,44]. In Europe and the United States, broad-spectrum insecticides (e.g., organophosphates, carbamates, pyrethroids, spinosyns and diamides) have been shown to be effective [6,45–50]. In this effort, it is important to reduce the amount of used pesticides while maintaining their effectiveness in order to limit the residues on fruits [51] and the development of insecticide resistance in the SWD [42,52].

## 2. Materials and Methods

### 2.1. CS-LC Nanoparticles

#### 2.1.1. Materials

Lambda-cyhalothrin 97% technical grade was purchased from Orient Resources International Co., Ltd. (ORICO), Zhuhai, Guangdong, China. Chitosan of high and low molecular weights, sodium tripolyphosphate, sodium alginate and Tween 80 were purchased from Sigma-Aldrich, Milan, Italy. Karate-zeon® 10% CS was provided by Syngenta, Milan, Italy. Sucrose was obtained from El-Gomhoria Co., Alexandria, Egypt. All used reagents were of analytical grade.

### 2.1.2. Experimental Design

An experimental  $2^{4-1}$  fractional factorial design was tailored to evaluate and optimize the effect of the formulation variables on the physicochemical properties of the CS-LC nanoparticles [53]. The fractional factorial design reduced considerably the number of preparations (from 16 preparations to 8, in the present case of four factors at two levels each), which is economic and time saving [54]. The four factors were CS molecular weight (MW) type, cross-linking agent, pesticide concentration and stirring rate, each at two levels (low and high) as shown in Table 1. The compositions of the designed formulations are shown in Table 2.

**Table 1.** Factors and levels of factorial design.

| Independent Variables            | Levels                 |                        |
|----------------------------------|------------------------|------------------------|
|                                  | Low                    | High                   |
| CS type (0.4% <i>w/v</i> )       | Low MW                 | High MW                |
| Cross-linking agent              | TPP (0.3% <i>w/v</i> ) | ALG (0.2% <i>w/v</i> ) |
| LC concentration (% <i>w/v</i> ) | 1                      | 1.5                    |
| Stirring rate (rpm)              | 500                    | 1500                   |

**Table 2.** Compositions of lambda-cyhalothrin nanoparticles.

| Formula Code | CS MW | Cross-Linking Agent (% <i>w/v</i> ) | Pesticide Conc (% <i>w/v</i> ) | Stirring Rate (rpm) |
|--------------|-------|-------------------------------------|--------------------------------|---------------------|
| F1           | High  | TPP (0.3)                           | 1.5                            | 1500                |
| F2           | High  | TPP (0.3)                           | 1                              | 500                 |
| F3           | Low   | TPP (0.3)                           | 1.5                            | 1500                |
| F4           | Low   | TPP (0.3)                           | 1                              | 500                 |
| F5           | High  | Alginate (0.2)                      | 1.5                            | 1500                |
| F6           | High  | Alginate (0.2)                      | 1                              | 500                 |
| F7           | Low   | Alginate (0.2)                      | 1.5                            | 1500                |
| F8           | Low   | Alginate (0.2)                      | 1                              | 500                 |

### 2.1.3. Preparation of CS-LC Nanoparticles

The nanoparticles were prepared using the ionotropic gelation technique previously described in [55–58]. Firstly, CS (high or low molecular weight) at 0.4% *w/v* was dissolved in 1% *v/v* acetic acid solution and kept overnight at room temperature to allow amino group formation [59–61]. Tween 80 (1% *v/v*) was added into the solution as a surfactant to reduce the nanoparticles' hydrodynamic diameter [61]. The core material (LC powder) was added to CS solutions under magnetic stirring until homogenous CS-LC dispersions were obtained. Cross-linking agent solutions of TPP and ALG were separately prepared in distilled water [60]. Nanoparticles were formed instantaneously upon the dropwise addition of the cross-linking solution to CS-LC dispersions under continuous gentle stirring for 60 min. Sucrose (5% *w/v*) was added to the prepared nanosuspension to act as a cryoprotectant. The nanoparticles were separated by cooling centrifugation at 20,000 rpm at 4 °C for 30 min, followed by freeze-drying at 20 Pa and −50 °C for 24 h (Freeze-drier Alpha 1–2 LD Martin-Christ-Germany).

## 2.2. Characterization of Nanoparticles

### 2.2.1. Physical Properties

#### Yield Percentage, Pesticide Loading and Entrapment Efficiency

The lyophilized LC-CS nanoparticles were weighed and referenced against the weight of the initial components according to the following equation:

$$\text{Yield percentage (\%YP)} = \frac{\text{Weight of nanoparticles}}{\text{Total initial solids weight}} \times 100 \quad (1)$$

The percent pesticide loading (%PL) refers to percentage of pesticide relative to amount of solid polymer, calculated as follows:

$$\%PL = \frac{\text{Amount of pesticide entrapped}}{\text{Total weight of polymer incorporated}} \times 100 \quad (2)$$

The percentage of entrapment efficiency (%EE) was determined by the direct method previously described in [62]. Five milligrams of CS-LC nanoparticles were dissolved in 20 mL of 1% *v/v* acetic acid and kept in an incubator overnight to allow for complete dissolution of CS. The precipitated LC residue was firstly separated by decantation of the supernatant CS solution and then dissolved in 10 mL of methanol. The concentration of LC was measured spectrophotometrically at  $\lambda_{\text{max}}$  278 nm (Spectrophotometer, Jasco, Tokyo, Japan). The %EE was then calculated using the following equation.

$$\%EE = \frac{\text{Amount of LC actually present}}{\text{Total amount of LC added}} \times 100 \quad (3)$$

#### Particle Size, Polydispersity Index and Zeta Potential

Based on the dynamic light scattering technique, the particle size, polydispersity index (PDI) and zeta potential of the developed formulas were measured by photon correlation spectroscopy (Zetasizer, Malvern Panalytical Ltd., Malvern, UK). A sample of the developed nanoparticles was mixed with 10 mL distilled water. All the samples were sonicated for 5 min prior to determination. All measurements were taken as an average of a triplicate.

### 2.2.2. Morphological and FTIR Examination

Transmission electron microscope (TEM; JEOL, JEM-1230, Akishima, Tokyo, Japan) analysis was performed to examine the morphological characteristics of the LC nanoparticles. The samples were diluted appropriately with 0.1 M phosphate buffer to capture the particles' image. The structural features of nanoparticles were measured by a Fourier transform infrared (FTIR) spectrometer (FTIR- 4100<sup>®</sup>, Jasco, Tokyo, Japan using KBr pellets [55].

### 2.3. In Vitro Release Study

The release of LC from the developed nanoparticles was tested in distilled water, using a modified USP apparatus-I dissolution tester (Hanson research SR6 dissolution tester, Hanson Research Corp., Chatsworth, CA, USA). A specified weight of each sample equivalent to 5 mg LC was placed in 100 mL dissolution medium at room temperature, 25 °C, and a stirring rate of 50 rpm. At predetermined time intervals, 1 mL of dissolution medium was withdrawn and replaced by the same volume of fresh media. The concentration of LC in the collected samples was measured spectrophotometrically at  $\lambda_{\text{max}}$  278 nm. The release study was performed in triplicate for each sample for a period of 6 h.

To examine the kinetics of LC release from the prepared nanoparticles, the release data were fitted to models representing zero-order, first-order and Higuchi's models. The correlation coefficient ( $R^2$ ) values were calculated from the plots of  $Q$  vs.  $t$  for zero-order,  $\log(Q_0 - Q)$  vs.  $t$  for first-order and  $Q$  vs.  $t^{1/2}$  for Higuchi;  $Q$  is the amount of pesticide released at time  $t$ , and  $(Q_0 - Q)$  is the amount of the pesticide remaining after time  $t$  [63,64].

## 2.4. Bioactivity of Nanoparticles

### 2.4.1. Laboratory SWD Colony

*Drosophila suzukii* used in the experiments originated from wild specimens from Northern Italy collected in the autumn of 2016. Mixed-sex adults were placed in 50 mL plastic culture vials (diameter 30 mm, length 115 mm) with ~15 mL specific medium for *D. suzukii* rearing (Bloomington Drosophila Stock Centre, Indiana University) [5,48–50]. Cultures were maintained in climate chambers at  $23 \pm 1$  °C,  $70 \pm 10\%$  R.H. and 16:8 h L:D regime. Wild *D. suzukii* adults were introduced into the colony on multiple occasions in 2017 and 2018 to ensure that the genetic make-up of the individuals screened in the laboratory was representative of the field population.

### 2.4.2. Laboratory Bioassays

Karate-zeon<sup>®</sup> (lambda cyhalothrin 10% w/v) was applied as a standard at its recommended label rate of application ( $25 \text{ mL h L}^{-1}$ ). For accurate comparison, the amount from each formulation containing 10% LC w/v was calculated according to the %PL of each formula. Ten treatments including the eight developed formulations, Karate-zeon and control (water) were evaluated. The experiment was arranged in a randomized complete block design, with 10 replicates for each treatment. A dipping non-infested fruit bioassay was used following the method described in Shower et al. (2018) [49], Cuthbertson, et al. [65]. Strawberries used for the bioassay were collected from insecticide-free orchards located in Verona province, Northeast Italy. Strawberries were previously tested for pesticide residues by exposing some fruit samples to adult SWDs for 24 h (h), and those with evidence of active pesticide residue (>5% mortality after 24 h exposure) were discarded. The fruits were completely dipped in the treatments for 30 s, dried and placed into 10 cm diameter ventilated plastic pots. Ten *D. suzukii* flies (five males + five females) were introduced into each plastic pot containing treated fruits. The pots were then maintained throughout the experimental period under controlled environmental conditions ( $23 \pm 1$  °C, 70% RH and 16 L: 8 D photoperiod). The mortality of *D. suzukii* adults was recorded at 4 and 16 h after treatment.

## 2.5. Statistical Analysis

Data of adult mortality were statistically analyzed by the generalized linear model (GLM) using one-way analysis of variance (ANOVA) followed by means separation with Tukey's least significant difference (LSD) test using JMP software version 4.0.4 (SAS Institute Inc., Cary, NC, USA). The percentages of SWD adult mortality were transformed to arcsine (sqrt (%mortality)) before analysis to stabilize variance, and reported means were back-transformed to percentages for presentation. Differences were considered significant at  $\alpha = 0.05$ .

## 3. Results

### 3.1. Characterizations of Nanoparticles

#### 3.1.1. Physical Properties

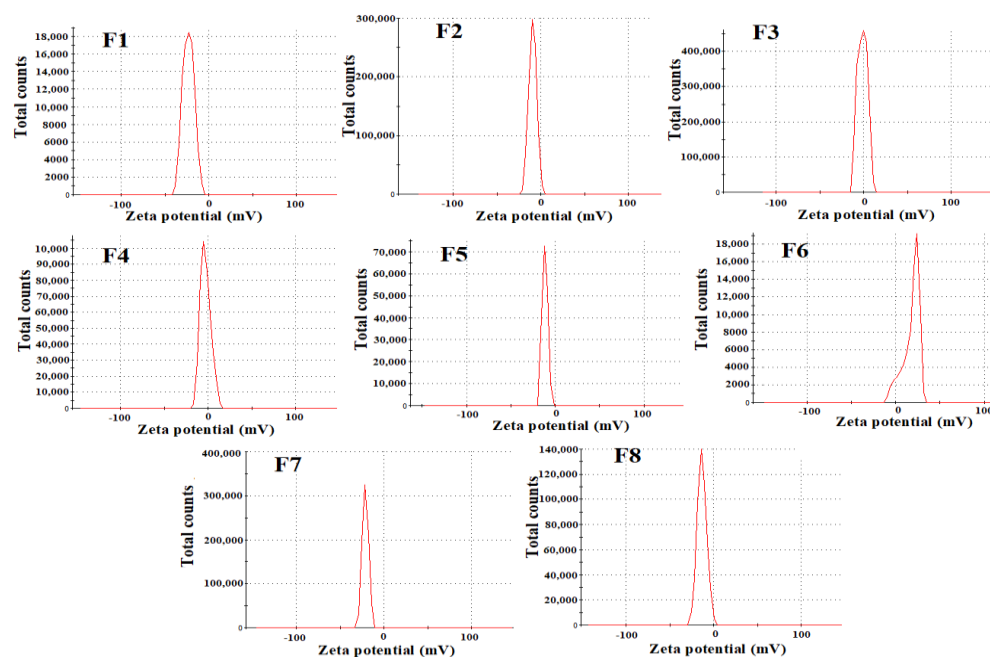
The %yield ranged from 50 to 80% for all preparations (Table 3). ANOVA results confirmed that the designed formulation variables showed a significant effect ( $p < 0.01$ ) on the yielded nanoparticles of all formulations. All formulations prepared with the high stirring rate (1500 rpm) showed higher yield percentages than those prepared with the low stirring rate (500 rpm).

**Table 3.** Physical characterization of CS-LC nanoparticles and desirability values showing the optimum formula.

| Formula | %Yield      | %PL         | %EE         | Particle Size (nm) | PDI          | Z-Potential (mv) | Desirability |
|---------|-------------|-------------|-------------|--------------------|--------------|------------------|--------------|
| F1      | 79.64 ± 2.1 | 10.86 ± 0.3 | 53.12 ± 3.5 | 346.1 ± 5.59       | 0.528 ± 0.05 | −23.1 ± 0.5      | 0.5511       |
| F2      | 58.44 ± 3.1 | 10.15 ± 0.9 | 68.93 ± 2.9 | 414.3 ± 14.2       | 0.448 ± 0.08 | −9.13 ± 0.3      | 0.5506       |
| F3      | 61.62 ± 1.7 | 9.8 ± 0.1   | 46.53 ± 3.9 | 308.4 ± 19.5       | 0.341 ± 0.03 | −1.21 ± 0.3      | 0.5511       |
| F4      | 57.31 ± 2.0 | 3.9 ± 0.2   | 24.95 ± 1.3 | 363 ± 27.7         | 0.457 ± 0.06 | −2.84 ± 0.3      | 0.5410       |
| F5      | 68.55 ± 3.2 | 8.41 ± 0.1  | 59.56 ± 2.1 | 353.3 ± 24.9       | 0.390 ± 0.05 | −11.3 ± 0.2      | 0.4801       |
| F6      | 57.48 ± 1.9 | 10.72 ± 0.4 | 73.56 ± 4.3 | 415.7 ± 22.8       | 0.447 ± 0.05 | −19.8 ± 0.6      | 0.4668       |
| F7      | 65.60 ± 2.5 | 4.15 ± 0.3  | 29.32 ± 1.2 | 278 ± 15.1         | 0.472 ± 0.01 | −21.1 ± 1.2      | 0.4967       |
| F8      | 59.29 ± 4.0 | 5.31 ± 0.1  | 36.12 ± 1.1 | 289 ± 19.1         | 0.453 ± 0.03 | −13.2 ± 0.5      | 0.4665       |

The %PL and %EE of the prepared formulations were significantly affected by the molecular weight of CS ( $p = 0.0046$ ) (Table 3). The formulations prepared with high MW CS cross-linked with either TPP or ALG showed higher %PL and %EE than those formulated with low MW CS. An inverse relationship between LC concentration and %PL or %EE was shown, except the case of CS with low MW/TPP (F3 and F4).

The respective average diameters of LC-loaded CS nanoparticles ranged from 278 to 415.7 nm (Table 3 and Supplementary Figure S1). The formula coded F7 (low MW CS cross-linked with ALG under low stirring at 500 rpm) showed the least particle size (278 nm) among the formulations. Formulas F7 and F8, both prepared by CS with low MW cross-linked with ALG, showed the lowest nanoparticle sizes (278 and 289 nm, respectively). The results showed low significant effect for the formulation variables on the particle size of LC-CS nanoparticles ( $p = 0.057$ ). However, ANOVA showed a significant effect of CS MW and LC concentration on PDI. All formulations showed  $PDI \leq 0.5$ , indicating homogeneity and a narrow range of distribution between particles. The results (Figure 1) demonstrated zeta potentials ranging between −2.3 and −23.1 mV. The formulas coded F1, F7, F6 and F2 showed the highest zeta potentials ( $> -19$ ). F4 and F3 showed low zeta potentials ( $< 5.7$ ).

**Figure 1.** Zeta potentials of prepared LC-CS nanoparticles.

Overall, both F1 and F3 showed the highest desirability, yielding the same value of 0.5511 (Table 3). They were followed by F2 (0.5506), F4 (0.5410), F7 (0.4967), F5 (0.4801),

F6 (0.4668) and F8 (0.4665). These results indicate the recommendation of F1 and F3 as optimum pesticide formulations. Moreover, the formulations F1, F3, F2 and F4 showed the four highest desirability values ( $\geq 0.5410$ ).

### 3.1.2. Morphological Characterization

In the present study, SEM and TEM images have shown the morphological properties and surface appearance of the fabricated nanoparticles. Figure 2 shows the SEM and TEM images of F3 and F5 as models for LC-CS nanoparticles cross-linked with TPP and ALG, respectively. The obtained nanoparticles had nearly spherical shape and a smooth surface, with a wide range of particle sizes (90–400 nm).

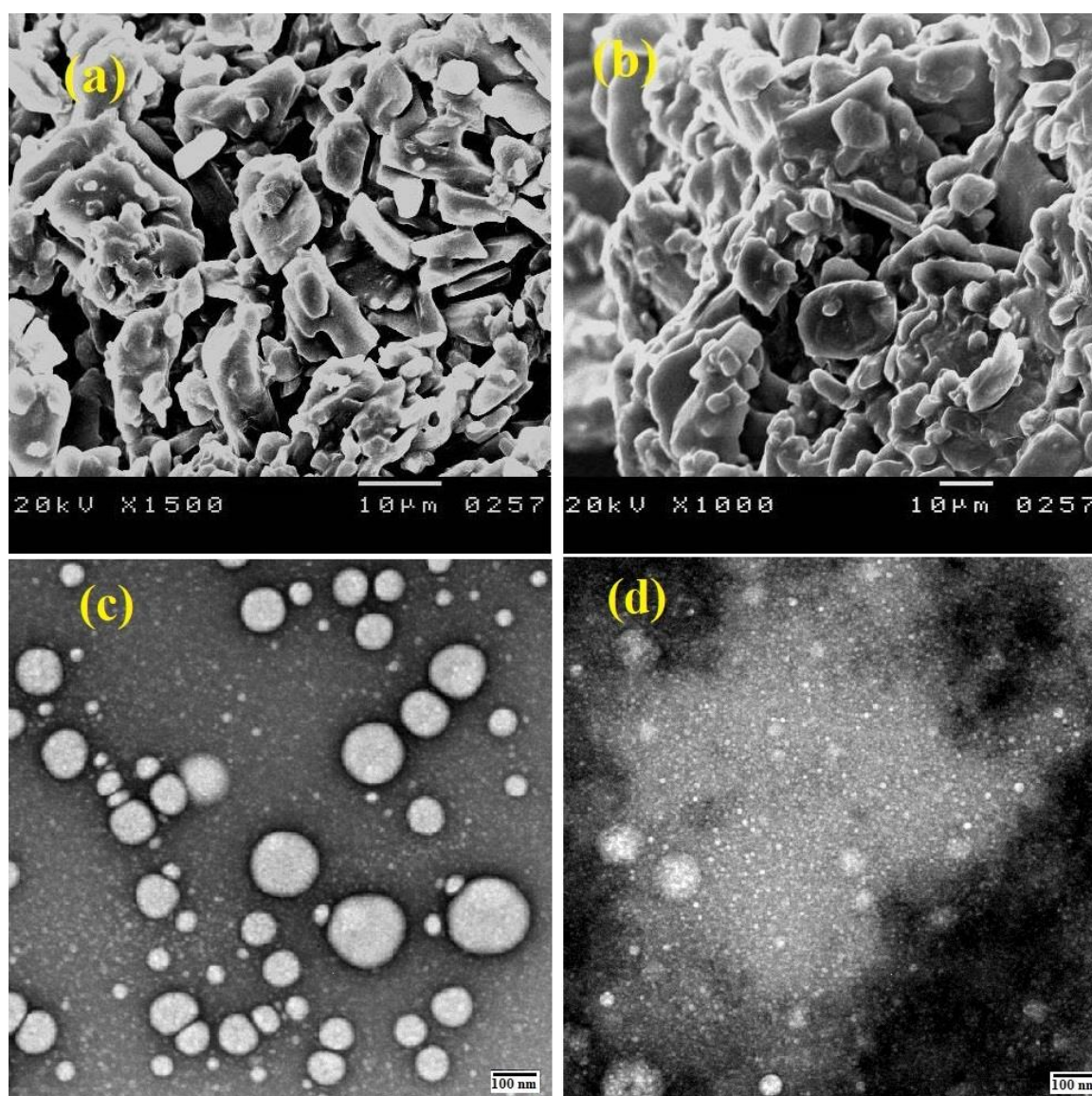


**Figure 2.** SEM and TEM images for LC-CS nanoparticles cross-linked with TPP (a,c) and TEM and SEM images (b,d) for LC-CS nanoparticles cross-linked with ALG.

### 3.1.3. FTIR Analysis

The FTIR spectra of CS, LC and LC-loaded CS nanoparticles were studied (Figure 3). Regarding the spectrum of LC, the peak appearing at  $3068\text{ cm}^{-1}$  is attributed to C-H bonds in the aromatic ring; however, C-H bonds in the aliphatic chain presented at  $2900\text{--}3000\text{ cm}^{-1}$ , and the sharp peak at  $1726\text{ cm}^{-1}$  is assigned to the C=O of LC; an-

other two peaks at 1647 and 1587  $\text{cm}^{-1}$  are attributed to C=C groups [66]. Furthermore, the peaks at 1077 and 800  $\text{cm}^{-1}$  are ascribed to the  $\text{CF}_3$  and V-Cl groups of LC. In the CS spectrum, the strong and wide peak at 3424  $\text{cm}^{-1}$  is attributed to the O-H stretching vibration, while the peak at 1635  $\text{cm}^{-1}$  is assigned the  $\text{CONH}_2$  group, and the peak at 2928  $\text{cm}^{-1}$  corresponds to the  $\text{CH}_2$  group. In the spectrum of CS-TPP nanoparticles (F3), the tip of the peak at 3424  $\text{cm}^{-1}$  of the CS spectrum was shifted to a lower wavenumber. Also, the peak for the N-H bending vibration of the amide II carbonyl stretch at 1650  $\text{cm}^{-1}$  in CS was shifted and overlapped with the peak of the C=O bond of LC at 1586.5  $\text{cm}^{-1}$ . These results can be attributed to the linkage between phosphoric and ammonium ions. In the ALG/CS nanoparticles spectrum (F5), the peak for the N-H bending vibration of the amide II carbonyl stretch at 1647.8  $\text{cm}^{-1}$  in CS of high MW was shifted and overlapped with the peak of the C=O bond of LC at 1586.5  $\text{cm}^{-1}$ ; this can be attributed to CS and ALG cross-linking. Overall, the characteristic peaks of LC were not affected by encapsulation in CS nanoparticles, as shown in Figure 4, indicating high compatibility between LC and other excipients. The obtained FTIR spectra of LC in the lower region ( $<3000 \text{ cm}^{-1}$ ) are similar, yet a few prominent changes were observed in the higher region ( $>3000 \text{ cm}^{-1}$ ). The broad bands at 3426  $\text{cm}^{-1}$  were flattened and shifted to 3390 and 3391  $\text{cm}^{-1}$ , respectively, in F3 and F5. These results confirm the successful cross-linking of CS nanoparticles as well as the successful loading of LC into CS.

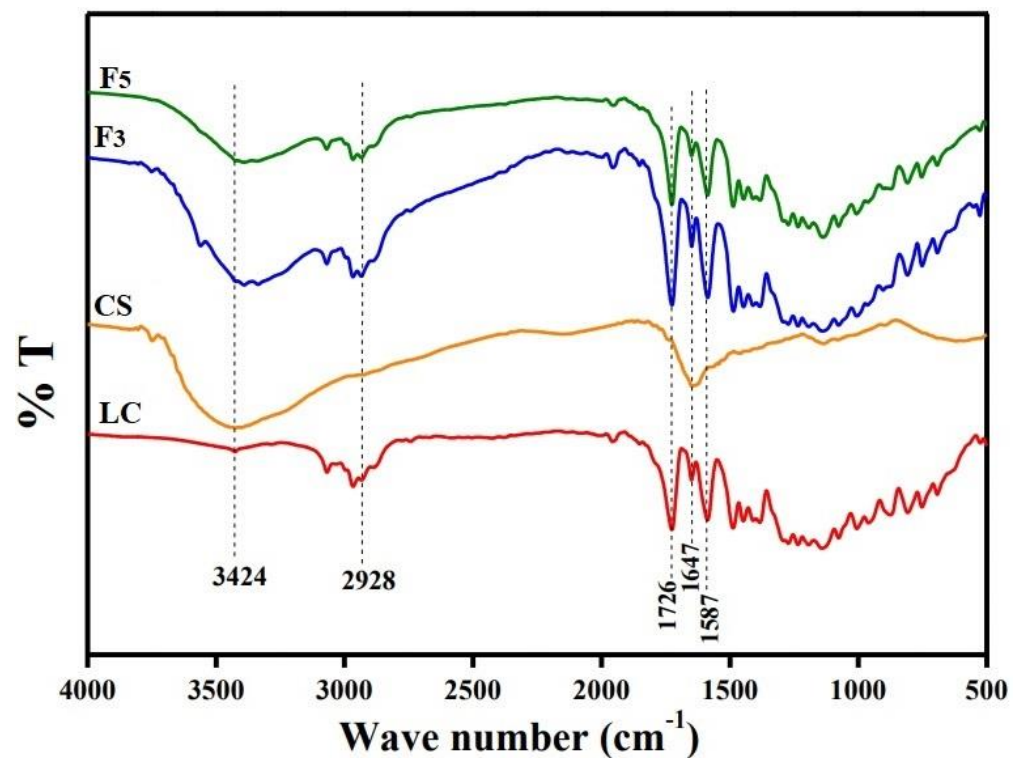


**Figure 3.** FTIR spectra of LC, CS, CS/TPP-loaded LC nanoparticles (F3) and CS/ALG-loaded LC nanoparticles (F5).



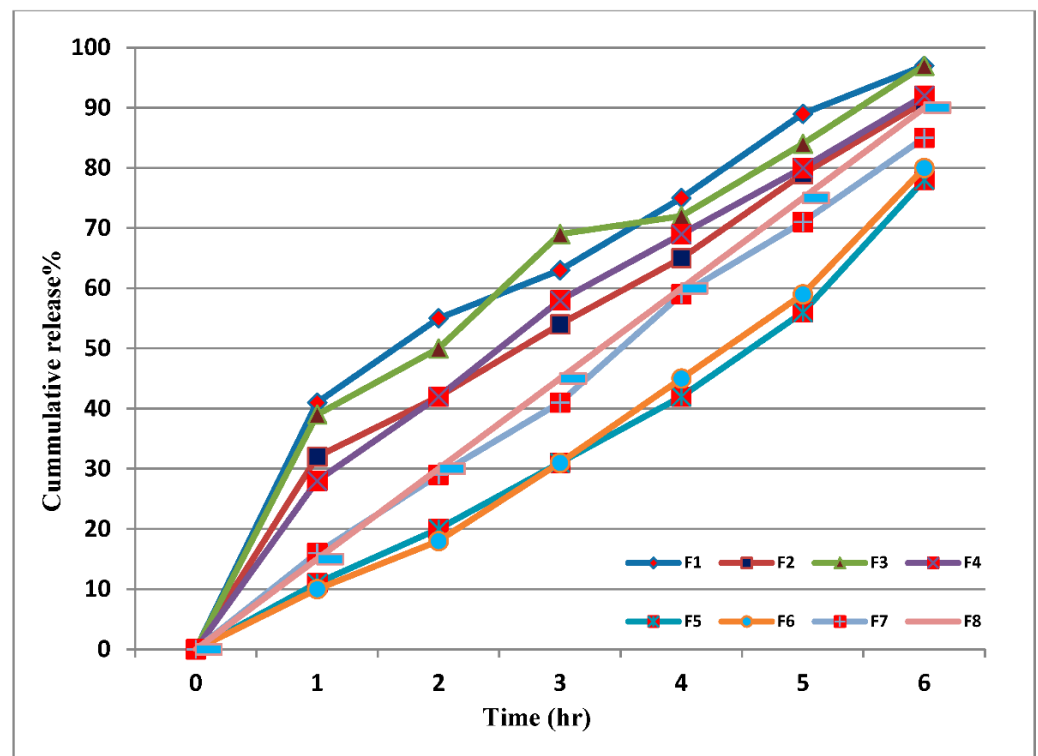


**Figure 4.** LC release profile from prepared LC-loaded CS nanoparticles (F1 to F8).

### 3.2. In Vitro Release Study

The release profile of LC-loaded CS nanoparticles cross-linked with TPP exhibited an initial burst release of about 30–40% in the first hour compared to only 10–15% drug release from ALG-cross-linked nanoparticles. However, our observations showed that about 90% of the loaded LC was released within 6 h of incubation in distilled water for all formulas (Figure 4). However, the release profile of LC-loaded CS nanoparticles cross-linked with ALG showed a constant sustained release of the pesticide during the time of the release study.

All the release profiles fit the zero order, which proved the ability of the nanoparticles to encapsulate LC and retard its release until sustainability was reached. The release of LC following the zero order may be due to the diffusion of encapsulated pesticide from the nanoparticle after erosion of its wall by the medium.

### 3.3. Bioactivity of Nanoparticles

All prepared formulations and Karate-zeon<sup>®</sup> significantly caused *D. sukuzii* mortality higher than the control at 2 HAT (male:  $F = 12.91$ ,  $DF = 9$ ,  $p < 0.0001$ ; Female:  $F = 14.82$ ;  $DF = 9$ ;  $p < 0.0001$ ) and at 16 HAT (males:  $F = 327.26$ ,  $DF = 9$ ,  $p < 0.0001$ ; females:  $F = 180.90$ ;  $DF = 9$ ;  $p < 0.0001$ ) (Table 4). The results revealed that the prepared formulations provided percent adult mortality higher than Karate-zeon<sup>®</sup> at 2 HAT (except F4 and F5 in females) and at 16 HAT (with statistical differences in females). The highest mortality was exhibited by F3 and F7, with both showing low particle sizes (304 and 278 nm, respectively) among the formulations; therefore, it could be concluded that there is a relationship between the particle size and the biological performance of the prepared nano-formulations.

**Table 4.** Percent mortality ( $\pm$ standard deviation) of male and female *D. suzukii* exposed to residual strawberries treated with CS-LC nanoparticles. Means within each column (time-gender) followed by the same letter (s) are not significantly different (Tukey's LSD test;  $p = 0.05$ ).

| Formula     | Percent Mortality |                   |                  |                  |
|-------------|-------------------|-------------------|------------------|------------------|
|             | 2 h               |                   | 16 h             |                  |
|             | Male              | Female            | Male             | Female           |
| F1          | 74.0 $\pm$ 5.8 a  | 78.0 $\pm$ 8.7 ab | 100 $\pm$ 0.0 a  | 98.0 $\pm$ 2.0 a |
| F2          | 74.0 $\pm$ 7.9 ab | 86.0 $\pm$ 5.2 a  | 100 $\pm$ 0.0 a  | 100 $\pm$ 0.0 a  |
| F3          | 84.0 $\pm$ 6.0 ab | 79.0 $\pm$ 7.0 ab | 100 $\pm$ 0.0 a  | 100 $\pm$ 0.0 a  |
| F4          | 82.0 $\pm$ 6.3 ab | 70.9 $\pm$ 6.3 ab | 100 $\pm$ 0.0 a  | 100 $\pm$ 0.0 a  |
| F5          | 70.0 $\pm$ 9.1 ab | 60.0 $\pm$ 10.3 b | 100 $\pm$ 0.0 a  | 100 $\pm$ 0.0 a  |
| F6          | 68.0 $\pm$ 9.0 ab | 80.0 $\pm$ 4.2 a  | 100 $\pm$ 0.0 a  | 100 $\pm$ 0.0 a  |
| F7          | 86.0 $\pm$ 4.3 a  | 84.0 $\pm$ 5.0 a  | 100 $\pm$ 0.0 a  | 100 $\pm$ 0.0 a  |
| F8          | 78.0 $\pm$ 6.3 ab | 68.0 $\pm$ 7.4 ab | 100 $\pm$ 0.0 a  | 100 $\pm$ 0.0 a  |
| Karate-zeon | 64.0 $\pm$ 7.8 b  | 74.0 $\pm$ 6.0 ab | 98.0 $\pm$ 2.0 a | 90.0 $\pm$ 5.4 b |
| Control     | 2.0 $\pm$ 2.0 c   | 0.0 $\pm$ 0.0 c   | 12.0 $\pm$ 4.4 b | 10.0 $\pm$ 3.3 c |

#### 4. Discussion

In the present study, we encapsulated lambda-cyhalothrin in a CS-TTP/ALG matrix using the ionic gelation technique. Based on our knowledge, this is the first study to prepare LC nanoparticles with the ionic gelation technique. These results open the door to the possibility of preparing other pyrethroids as nano-pesticides via this technique. The formed cross-linking matrix controls the release of the pesticide's active ingredients. This conception was confirmed by Shen, et al. [67], who recorded significant differences in the release properties of LC nanoparticles. However, LC was previously prepared as a nano-pesticide using other methods such as the solvent evaporation and melt emulsification–high-pressure homogenization techniques. For example, Shen et al. [67] prepared LC nanoparticles by the solvent evaporation method utilizing polylactic acid as a carrier. They produced uniform-spherical and smooth-surface nanoparticles with a size of less than 200 nm. An acceptable LC-loading capacity (46.6%) and a high encapsulation efficiency (more than 90%) were obtained [67]. Pan, et al. [68] prepared LC 5% as a nanosuspension by the melt emulsification–high-pressure homogenization method, obtaining a mean particle size of  $16.01 \pm 0.11$  nm. In 2019, an LC nanosuspension was prepared by the one-step melt emulsification technique [69]. The produced particles had excellent properties with the smaller particle size ( $12.0 \pm 0.1$  nm) the researchers obtained.

We used a fractional factorial design to select the most suitable preparation variables to obtain the optimum formulation in terms of chemical and physical properties. It recommended the optimum formulas (with F1 and F3 giving the highest desirability values). The common formulation variables between both these formulations were the cross-linking agent (TTP), LC concentration (1.5% *w/v*) and stirring rate (1500 rpm). Moreover, the principle stable variable between the four formulations (F1, F3, F2 and F4) with the highest desirability values ( $\geq 0.5410$ ) was the cross-linking agent, TTP. These data reveal that TTP was more suitable than ALG as a cross-linking agent for preparing CS-LC nanoparticles. However, the presence of two polymers (CS and ALG) may have facilitated interaction, resulting in greater %EE [70]. The TEM photographs confirmed that loaded nanoparticles had nearly a uniform spherical shape and a smooth surface [67]. The FTIR spectra confirmed the cross-linkage between CS and the cross-linking agents (TTP or ALG). The stirring speed during ionic gelation significantly affected the reaction yield [71]. The nanoparticle sizes and PDI were significantly affected by the CS molecular weight [72]. The formulations prepared using low-MW CS had smaller particle sizes than these obtained with high-MW

CS. This may be attributed to the low viscosity of the low-MW CS used [72]. The prepared nanoparticle formulations provided activity against *D. suzukii* adults greater than that caused by a commercial product (Karate-zeon<sup>®</sup>) containing same active ingredient (LC).

The obtained results indicate that the bioactivity of LC nanoparticles against *D. suzukii* adults was affected by their particle size. The best activity of the prepared LC nanoparticles was caused by the formula with the smallest particle size (278 nm). Our results are in harmony with these previously obtained in [23,73–77]. Those findings have the potential to be very beneficial and applicable in the control of the SWD insect, which attacks fruits nearing harvest during the ripening period, when the use of chemical insecticides is critical. In such cases, reducing the pesticide application times is strongly encouraged in order to avoid exceeding the maximum residue limits on fruits. This can be accomplished by improving the biological performance of the insecticides used, reducing application times and chemical residues on fruits, lowering the negative effects on the environment and non-targeted organisms and delaying the development of insecticide resistance. Increasing the surface area and, therefore, the solubility, are two well-known benefits of using smaller particles [78,79]. Wang et al. [77] previously demonstrated that avermectin nano-delivery systems can significantly improve pesticides' controllable release, photostability and biological activity, thereby improving efficiency and reducing pesticide residues. The ionic gelation approach was used by Rajkumar et al. [76] to encapsulate peppermint oil in chitosan nanoparticles. It was reported that using nanoparticles considerably enhanced the oil's toxicity against the stored product pests *Sitophilus oryzae* (L.) and *Tribolium castaneum* (Herbst). In vivo, nanoparticles inhibited AChE activity in *S. oryzae* and *T. castaneum* by 52.43 and 37.80%, respectively, under optimal conditions. Paulraj et al. [75] developed CS-TPP nanoparticles loaded with a botanical pesticide, Ponneem<sup>®</sup>, a blend of seed oils of *Pongamia pinnata* and *Azadirachta indica*, and assessed its antifeedant, larvicidal and growth-regulation effects against *Helicoverpa armigera*, an important lepidopteran pest. The size of the nanoparticles (32 to 90 nm) was confirmed by electron micrography, and the cross-linking of chitosan with TPP was confirmed by FTIR spectroscopy. The nanoparticles evidenced 88.5 and 90.2% antifeedant and larvicidal activity against *H. armigera*, respectively. In addition, they reduced the weights of *H. armigera* pupae substantially.

The ability of the prepared nanoparticles to retard the release of LC in the agricultural environment was assessed by conducting a release study. The release profile of LC-loaded CS nanoparticles cross-linked with TPP exhibited an initial burst release of about 30–40% in the first hour, followed by a controlled release of 50–60% for the subsequent 5 h. The observed burst effect can be attributed to dissociation of LC molecules that were loosely bound to the surface of CS nanoparticles [55,80]. The second part of the release profile is related to the slow release of entrapped LC molecules at an approximately constant rate that arises from the slow degradation of the nanoparticles [55,81]. However, the release profile of LC-loaded CS nanoparticles cross-linked with ALG showed a constant sustained release of LC during the release study. This release behavior may be due to the high density of the nanoparticle core and also an increase in the diffusional path length, which the pesticide molecules have to traverse. Grillo, et al. [82] formulated chitosan nanoparticles loaded with the herbicide paraquat by modifying CS with TPP via the ionic gelation technique. Their kinetic release study revealed that the nanoparticles delayed the release time of paraquat compared to the free herbicide. Silva, et al. [83] also noted that nanoparticles prolonged the release of paraquat for 2 h longer than the free herbicide and attributed this to the strong interaction of paraquat with the nanoparticles, which could have an inhibitory effect on the release of the herbicide into the soil.

In summary, ionic gelation could be a potential method for preparing nanoparticles of LC or other pyrethroids for application in pest management, particularly in the home and in relation to public health. Nanoparticles, on the other hand, should be studied more thoroughly in terms of their environmental impact.

## 5. Conclusions

It could be concluded that there is a significant relationship between the particle size and the biological performance of the nano-formulations. The encapsulating of chemical pesticides in biodegradable polymers such as chitosan is a promising approach in sustainable agriculture due to its improving their potential activity in target pests, reducing concentration or application times and/or rates of used chemicals and in turn decreasing the toxicity to human, non-targeted organisms and the risk of wider environmental contamination.

**Supplementary Materials:** The following supporting information can be downloaded at: <https://www.mdpi.com/article/10.3390/nano12183110/s1>, Figure S1: Respective average diameters of LC-loaded CS nanoparticles.

**Author Contributions:** Conceptualization, R.S. and N.M.; methodology, R.S., E.S.E.-L., R.S.A.-R. and N.M.; software, R.S., A.S.E., E.S.E.-L., R.S.A.-R. and R.S.B.; formal analysis, R.S., A.S.E., R.S.B. and E.S.E.-L.; investigation, R.S., R.S.A.-R. and N.M.; resources, R.S., R.S.B., R.S.A.-R. and A.S.E.; writing—original draft preparation, R.S., R.S.B., R.S.A.-R. and A.S.E.; writing—review and editing, R.S., R.S.B. and N.M.; visualization, R.S., R.S.A.-R., A.S.E. and N.M.; supervision, R.S. and N.M. All authors have read and agreed to the published version of the manuscript.

**Funding:** This research was funded by the European Union's Seventh Framework Programme for research, technological development and demonstration under grant agreement number 613678, as a part of the project on strategies to develop effective, innovative and practical approaches to protect major European fruit crops from pests and pathogens (DROPSA).

**Institutional Review Board Statement:** Not applicable.

**Informed Consent Statement:** Not applicable.

**Data Availability Statement:** Not applicable.

**Conflicts of Interest:** The authors declare no conflict of interest.

## References

1. Sharma, S.; Kooner, R.; Arora, R. Insect pests and crop losses. In *Breeding Insect Resistant Crops for Sustainable Agriculture*; Springer: Berlin/Heidelberg, Germany, 2017; pp. 45–66.
2. Ebadollahi, A.; Jalali Sendi, J.; Setzer, W.N.; Changbunjong, T. Encapsulation of Eucalyptus largiflorens Essential Oil by Mesoporous Silicates for Effective Control of the Cowpea Weevil, *Callosobruchus maculatus* (Fabricius) (Coleoptera: Chrysomelidae). *Molecules* **2022**, *27*, 3531. [[CrossRef](#)] [[PubMed](#)]
3. Ebadollahi, A.; Naseri, B.; Abedi, Z.; Setzer, W.N. Chemical Profiles and Insecticidal Potential of Essential Oils Isolated from Four Thymus Species against *Rhyzopertha dominica* (F.). *Plants* **2022**, *11*, 1567. [[CrossRef](#)] [[PubMed](#)]
4. Haye, T.; Girod, P.; Cuthbertson, A.; Wang, X.; Daane, K.; Hoelmer, K.; Baroffio, C.; Zhang, J.; Desneux, N. Current SWD IPM tactics and their practical implementation in fruit crops across different regions around the world. *J. Pest Sci.* **2016**, *89*, 643–651. [[CrossRef](#)]
5. Shower, R.; Donati, I.; Cellini, A.; Spinelli, F.; Mori, N. Insecticidal Activity of *Photorhabdus luminescens* against *Drosophila suzukii*. *Insects* **2018**, *9*, 148. [[CrossRef](#)] [[PubMed](#)]
6. Shower, R. Chemical control of *Drosophila suzukii*. In *Drosophila suzukii Management*; Springer: Berlin/Heidelberg, Germany, 2020; pp. 133–142.
7. Shower, R.; El-Shazly, M.M.; Khider, A.M.; Baeshen, R.S.; Hikal, W.M.; Kordy, A.M. Botanical Oils Isolated from *Simmondsia chinensis* and *Rosmarinus officinalis* Cultivated in Northern Egypt: Chemical Composition and Insecticidal Activity against *Sitophilus oryzae* (L.) and *Tribolium castaneum* (Herbst). *Molecules* **2022**, *27*, 4383. [[CrossRef](#)]
8. Enkerli, J.; Widmer, F.; Keller, S. Long-term field persistence of *Beauveria brongniartii* strains applied as biocontrol agents against European cockchafer larvae in Switzerland. *Biol. Control* **2004**, *29*, 115–123. [[CrossRef](#)]
9. Sahayaraj, K.; Namasivayam, S.K.R. Mass production of entomopathogenic fungi using agricultural products and by products. *Afr. J. Biotechnol.* **2008**, *7*, 1907–1910.
10. Karungi, J.; Kyamanywa, S.; Adipala, E.; Erbaugh, M. Pesticide utilisation, regulation and future prospects in small scale horticultural crop production systems in a developing country. In *Pesticides in the Modern World-Pesticides Use and Management*; InTech: Rijeka, Croatia, 2011. [[CrossRef](#)]
11. Shower, R.; Abou-Elnasar, H.; El-Dardir, M.M.; Kordy, A.M. Biochemical and Toxicological Effects of Emamectin Benzoate against *Spodoptera littoralis* (Boisd.) (Lepidoptera: Noctuidae). *Egypt. Acad. J. Biol. Sci. F. Toxicol. Pest Control* **2022**, *14*, 1–11. [[CrossRef](#)]

12. Ismail, I.A.; Qari, S.H.; Shower, R.; Elshaer, M.M.; Dessoky, E.S.; Youssef, N.H.; Hamad, N.A.; Abdelkhalek, A.; Elsamra, I.A.; Behiry, S.I. The Application of Pomegranate, Sugar Apple, and Eggplant Peel Extracts Suppresses *Aspergillus flavus* Growth and Aflatoxin B1 Biosynthesis Pathway. *Horticulturae* **2021**, *7*, 558. [CrossRef]
13. Shower, R.; El-Shazly, M.M.; Khider, A.M.; Kordy, A.M. Chemical Composition of Five Botanical Powders and Their Insecticidal Activity Against the Rice Weevil, *Sitophilus oryzae* on Wheat Crop. *Egypt. Acad. J. Biol. Sci. G. Microbiol.* **2020**, *12*, 125–136. [CrossRef]
14. Sundar, N.S.; Karthi, S.; Sivanesh, H.; Stanley-Raja, V.; Chanthini, K.M.-P.; Ramasubramanian, R.; Ramkumar, G.; Ponsankar, A.; Narayanan, K.R.; Vasantha-Srinivasan, P. Efficacy of Precocene I from *Desmosstachya bipinnata* as an Effective Bioactive Molecules against the *Spodoptera litura* Fab. and Its Impact on *Eisenia fetida* Savigny. *Molecules* **2021**, *26*, 6384. [CrossRef] [PubMed]
15. Singh, S.; Mukherjee, A.; Jaiswal, D.K.; de Araujo Pereira, A.P.; Prasad, R.; Sharma, M.; Kuhad, R.C.; Shukla, A.C.; Verma, J.P. Advances and future prospects of pyrethroids: Toxicity and microbial degradation. *Sci. Total Environ.* **2022**, *829*, 154561. [CrossRef] [PubMed]
16. Chrustek, A.; Holyńska-Iwan, I.; Dziembowska, I.; Bogusiewicz, J.; Wróblewski, M.; Cwynar, A.; Olszewska-Słonina, D. Current research on the safety of pyrethroids used as insecticides. *Medicina* **2018**, *54*, 61. [CrossRef] [PubMed]
17. KB, A.A.; HM, A.R. Lambda, the pyrethroid insecticide as a mutagenic agent in both somatic and germ cells. *J. Am. Sci.* **2010**, *6*, 317–326.
18. Guida, Y.; Pozo, K.; de Carvalho, G.O.; Capella, R.; Targino, A.C.; Torres, J.P.M.; Meire, R.O. Occurrence of pyrethroids in the atmosphere of urban areas of Southeastern Brazil: Inhalation exposure and health risk assessment. *Environ. Pollut.* **2021**, *290*, 118020. [CrossRef]
19. Zaim, M.; Aitio, A.; Nakashima, N. Safety of pyrethroid-treated mosquito nets. *Med. Vet. Entomol.* **2000**, *14*, 1–5. [CrossRef]
20. Gnanguenon, V.; Agossa, F.R.; Badirou, K.; Govoetchan, R.; Anagonou, R.; Oke-Agbo, F.; Azondekon, R.; AgbanrinYousouf, R.; Attolou, R.; Tokponnon, F.T. Malaria vectors resistance to insecticides in Benin: Current trends and mechanisms involved. *Parasites Vectors* **2015**, *8*, 223. [CrossRef]
21. He, L.-M.; Troiano, J.; Wang, A.; Goh, K. Environmental chemistry, ecotoxicity, and fate of lambda-cyhalothrin. In *Reviews of Environmental Contamination and Toxicology*; Springer: Berlin/Heidelberg, Germany, 2008; pp. 71–91.
22. IRAC, Insecticide Resistance Action Committee, IRAC Mode of Action Classification Scheme MOA CLASSIFICATION, Ver. 10.3. 2022. Available online: <https://irac-online.org/> (accessed on 1 June 2022).
23. Cui, B.; Feng, L.; Pan, Z.; Yu, M.; Zeng, Z.; Sun, C.; Zhao, X.; Wang, Y.; Cui, H. Evaluation of stability and biological activity of solid nanodispersion of lambda-cyhalothrin. *PLoS ONE* **2015**, *10*, e0135953. [CrossRef]
24. Kah, M.; Hofmann, T. Nanopesticide research: Current trends and future priorities. *Environ. Int.* **2014**, *63*, 224–235. [CrossRef]
25. Balaure, P.C.; Gudovan, D.; Gudovan, I. Nanopesticides: A new paradigm in crop protection. In *New Pesticides and Soil Sensors*; Elsevier: Amsterdam, The Netherlands, 2017; pp. 129–192.
26. Bharani, R.A.; Namasivayam, S.K.R.; Shankar, S.S. Biocompatible Chitosan Nanoparticles Incorporated Pesticidal Protein Beauvericin (Csnp-Bv) Preparation for the Improved Pesticidal Activity Against Major Groundnut Defoliator *Spodoptera litura* (Fab.)(Lepidoptera; Noctuidae). *Int. J. Chem.Tech. Res.* **2014**, *6*, 5007–5012.
27. Scott, N.R. *Nanotechnology Opportunities in Agriculture and Food Systems*; Biological & Environmental Engineering, University NSF Cornell Nanoscale Science & Engineering Grantees Conference: Arlington, VA, USA, 2007.
28. Bouwmeester, H.; Dekkers, S.; Noordam, M.Y.; Hagens, W.I.; Bulder, A.S.; De Heer, C.; Ten Voorde, S.E.; Wijnhoven, S.W.; Marvin, H.J.; Sips, A.J. Review of health safety aspects of nanotechnologies in food production. *Regul. Toxicol. Pharmacol.* **2009**, *53*, 52–62. [CrossRef] [PubMed]
29. Kashyap, P.L.; Xiang, X.; Heiden, P. Chitosan nanoparticle based delivery systems for sustainable agriculture. *Int. J. Biol. Macromol.* **2015**, *77*, 36–51. [CrossRef] [PubMed]
30. Abd El-Monaem, E.M.; Eltaweil, A.S.; Elshishini, H.M.; Hosny, M.; Abou Alsoaud, M.M.; Attia, N.F.; El-Subruiti, G.M.; Omer, A.M. Sustainable adsorptive removal of antibiotic residues by chitosan composites: An insight into current developments and future recommendations. *Arab. J. Chem.* **2022**, *15*, 103743. [CrossRef]
31. George, M.; Abraham, T.E. Polyionic hydrocolloids for the intestinal delivery of protein drugs: Alginate and chitosan—A review. *J. Control. Release* **2006**, *114*, 1–14. [CrossRef]
32. Stoica, R.; Şomoghi, R.; Ion, R. Preparation of Chitosan-Tripolyphosphate Nanoparticles for the Encapsulation of Polyphenols Extracted from Rose Hips. *Dig. J. Nanomater. Biostructures (DJNB)* **2013**, *8*, 955–963.
33. Hoang, N.H.; Le Thanh, T.; Sangpueak, R.; Treekoon, J.; Saengchan, C.; Thepbandit, W.; Papatthoti, N.K.; Kamkaew, A.; Buensanteai, N. Chitosan Nanoparticles-Based Ionic Gelation Method: A Promising Candidate for Plant Disease Management. *Polymers* **2022**, *14*, 662. [CrossRef] [PubMed]
34. Pedroso-Santana, S.; Fleitas-Salazar, N. Ionotropic gelation method in the synthesis of nanoparticles/microparticles for biomedical purposes. *Polym. Int.* **2020**, *69*, 443–447. [CrossRef]
35. Eltaweil, A.S.; Abd El-Monaem, E.M.; Elshishini, H.M.; El-Aqapa, H.G.; Hosny, M.; Abdelfatah, A.M.; Ahmed, M.S.; Hammad, E.N.; El-Subruiti, G.M.; Fawzy, M. Recent developments in alginate-based adsorbents for removing phosphate ions from wastewater: A review. *RSC Adv.* **2022**, *12*, 8228–8248. [CrossRef]
36. Bolda, M.P.; Goodhue, R.E.; Zalom, F.G. Spotted wing drosophila: Potential economic impact of a newly established pest. *Agric. Resour. Econ. Update* **2010**, *13*, 5–8.

37. Walsh, D.B.; Bolda, M.P.; Goodhue, R.E.; Dreves, A.J.; Lee, J.; Bruck, D.J.; Walton, V.M.; O'Neal, S.D.; Zalom, F.G. *Drosophila suzukii* (Diptera: Drosophilidae): Invasive pest of ripening soft fruit expanding its geographic range and damage potential. *J. Integr. Pest Manag.* **2011**, *2*, G1–G7. [[CrossRef](#)]
38. Goodhue, R.E.; Bolda, M.; Farnsworth, D.; Williams, J.C.; Zalom, F.G. Spotted wing drosophila infestation of California strawberries and raspberries: Economic analysis of potential revenue losses and control costs. *Pest Manag. Sci.* **2011**, *67*, 1396–1402. [[CrossRef](#)] [[PubMed](#)]
39. Deprá, M.; Poppe, J.L.; Schmitz, H.J.; De Toni, D.C.; Valente, V.L. The first records of the invasive pest *Drosophila suzukii* in the South American continent. *J. Pest Sci.* **2014**, *87*, 379–383. [[CrossRef](#)]
40. EPPO, EPPO Global Database. *Drosophila Suzukii*. 2018. Available online: <https://gd.eppo.int/taxon/DROSSU/distribution> (accessed on 18 May 2020).
41. Cini, A.; Ioriatti, C.; Anfora, G. A review of the invasion of *Drosophila suzukii* in Europe and a draft research agenda for integrated pest management. *Bull. Insectology* **2012**, *65*, 149–160.
42. Asplen, M.K.; Anfora, G.; Biondi, A.; Choi, D.-S.; Chu, D.; Daane, K.M.; Gibert, P.; Gutierrez, A.P.; Hoelmer, K.A.; Hutchison, W.D. Invasion biology of spotted wing *Drosophila* (*Drosophila suzukii*): A global perspective and future priorities. *J. Pest Sci.* **2015**, *88*, 469–494. [[CrossRef](#)]
43. Ioriatti, C.; Boselli, M.; Caruso, S.; Galassi, T.; Gottardello, A.; Grassi, A.; Tonina, L.; Vaccari, G.; Mori, N. Approccio integrato per la difesa dalla *Drosophila suzukii*. *Riv. Di Fruttic. E Di Ortofloric.* **2015**, *77*, 32–37.
44. Mori, N.; Tonina, L.; Sancassani, M.; Colombari, F.; Dall'Ara, P.; Cero, M.d.; Marchesini, E. Integrated pest management approaches against *Drosophila suzukii*. *Italus Hortus* **2019**, *26*, 67–74. [[CrossRef](#)]
45. Beers, E.H.; Van Steenwyk, R.A.; Shearer, P.W.; Coates, W.W.; Grant, J.A. Developing *Drosophila suzukii* management programs for sweet cherry in the western United States. *Pest Manag. Sci.* **2011**, *67*, 1386–1395. [[CrossRef](#)]
46. Bruck, D.J.; Bolda, M.; Tanigoshi, L.; Klick, J.; Kleiber, J.; DeFrancesco, J.; Gerdeman, B.; Spitler, H. Laboratory and field comparisons of insecticides to reduce infestation of *Drosophila suzukii* in berry crops. *Pest Manag. Sci.* **2011**, *67*, 1375–1385. [[CrossRef](#)]
47. Van Timmeren, S.; Isaacs, R. Control of spotted wing drosophila, *Drosophila suzukii*, by specific insecticides and by conventional and organic crop protection programs. *Crop Prot.* **2013**, *54*, 126–133. [[CrossRef](#)]
48. Shower, R.; Tonina, L.; Gariberti, E.; Mori, N. Efficacy of insecticides against *Drosophila suzukii* on cherries. In *XVIII. International Plant Protection Congress*; DPG: Berlin, Germany, 2015.
49. Shower, R.; Tonina, L.; Tirello, P.; Duso, C.; Mori, N. Laboratory and field trials to identify effective chemical control strategies for integrated management of *Drosophila suzukii* in European cherry orchards. *Crop Prot.* **2018**, *103*, 73–80. [[CrossRef](#)]
50. Shower, R. Impact of Traditional Pesticides and New Controlled Release Formulations on *Drosophila suzukii*. Ph.D. Thesis, Padova University, Padova, Italy, 2017.
51. Haviland, D.R.; Beers, E.H. Chemical control programs for *Drosophila suzukii* that comply with international limitations on pesticide residues for exported sweet cherries. *J. Integr. Pest Manag.* **2012**, *3*, F1–F6. [[CrossRef](#)]
52. Wiman, N.G.; Dalton, D.T.; Anfora, G.; Biondi, A.; Chiu, J.C.; Daane, K.M.; Gerdeman, B.; Gottardello, A.; Hamby, K.A.; Isaacs, R. *Drosophila suzukii* population response to environment and management strategies. *J. Pest Sci.* **2016**, *89*, 653–665. [[CrossRef](#)]
53. de Pinho Neves, A.L.; Milioli, C.C.; Müller, L.; Riella, H.G.; Kuhnen, N.C.; Stulzer, H.K. Factorial design as tool in chitosan nanoparticles development by ionic gelation technique. *Colloids Surf. A Physicochem. Eng. Asp.* **2014**, *445*, 34–39. [[CrossRef](#)]
54. Montgomery, J.D. Social networks and labor-market outcomes: Toward an economic analysis. *Am. Econ. Rev.* **1991**, *81*, 1408–1418.
55. Mohammadpour Dounighi, N.; Eskandari, R.; Avadi, M.; Zolfagharian, H.; Mir Mohammad Sadeghi, A.; Rezayat, M. Preparation and in vitro characterization of chitosan nanoparticles containing *Mesobuthus eupeus* scorpion venom as an antigen delivery system. *J. Venom. Anim. Toxins Incl. Trop. Dis.* **2012**, *18*, 44–52. [[CrossRef](#)]
56. Werle, M.; Takeuchi, H.; Bernkop-Schnürch, A. Modified chitosans for oral drug delivery. *J. Pharm. Sci.* **2009**, *98*, 1643–1656. [[CrossRef](#)]
57. Calvo, P.; Remunan-Lopez, C.; Vila-Jato, J.L.; Alonso, M. Novel hydrophilic chitosan-polyethylene oxide nanoparticles as protein carriers. *J. Appl. Polym. Sci.* **1997**, *63*, 125–132. [[CrossRef](#)]
58. Calvo, P.; Remuñan-López, C.; Vila-Jato, J.L.; Alonso, M.J. Chitosan and chitosan/ethylene oxide-propylene oxide block copolymer nanoparticles as novel carriers for proteins and vaccines. *Pharm. Res.* **1997**, *14*, 1431–1436. [[CrossRef](#)]
59. Gazori, T.; Khoshayand, M.R.; Azizi, E.; Yazdizade, P.; Nomani, A.; Haririan, I. Evaluation of Alginate/Chitosan nanoparticles as antisense delivery vector: Formulation, optimization and in vitro characterization. *Carbohydr. Polym.* **2009**, *77*, 599–606. [[CrossRef](#)]
60. Leelapornpisid, P.; Leesawat, P.; Natakarnkitkul, S.; Rattanapanadda, P. Application of chitosan for preparation of arbutin nanoparticles as skin whitening. *J. Met. Mater. Miner.* **2010**, *20*, 101–105.
61. Masalova, O.; Kulikouskaya, V.; Shutava, T.; Agabekov, V. Alginate and Chitosan gel nanoparticles for efficient protein entrapment. *Phys. Procedia* **2013**, *40*, 69–75. [[CrossRef](#)]
62. Açıkgöz, M.; Kaş, H.; Orman, M.; Hincal, A. Chitosan microspheres of diclofenac sodium: I. application of factorial design and evaluation of release kinetics. *J. Microencapsul.* **1996**, *13*, 141–159. [[CrossRef](#)] [[PubMed](#)]
63. Barzegar-Jalali, M. Kinetic analysis of drug release from nanoparticles. *J. Pharm. Pharm. Sci.* **2008**, *11*, 167–177. [[CrossRef](#)]
64. England, C.G.; Miller, M.C.; Kuttan, A.; Trent, J.O.; Frieboes, H.B. Release kinetics of paclitaxel and cisplatin from two and three layered gold nanoparticles. *Eur. J. Pharm. Biopharm.* **2015**, *92*, 120–129. [[CrossRef](#)]

65. Cuthbertson, A.G.; Collins, D.A.; Blackburn, L.F.; Audsley, N.; Bell, H.A. Preliminary screening of potential control products against *Drosophila suzukii*. *Insects* **2014**, *5*, 488–498. [[CrossRef](#)] [[PubMed](#)]
66. Hosny, M.; Fawzy, M.; El-Fakharany, E.M.; Omer, A.M.; Abd El-Monaem, E.M.; Khalifa, R.E.; Eltaweil, A.S. Biogenic synthesis, characterization, antimicrobial, antioxidant, antidiabetic, and catalytic applications of platinum nanoparticles synthesized from *Polygonum salicifolium* leaves. *J. Environ. Chem. Eng.* **2022**, *10*, 106806. [[CrossRef](#)]
67. Shen, Y.; Zhu, H.; Cui, J.; Wang, A.; Zhao, X.; Cui, B.; Wang, Y.; Cui, H. Construction of lambda-cyhalothrin nano-delivery system with a high loading content and controlled-release property. *Nanomaterials* **2018**, *8*, 1016. [[CrossRef](#)]
68. Pan, Z.; Cui, B.; Zeng, Z.; Feng, L.; Liu, G.; Cui, H.; Pan, H. Lambda-cyhalothrin nanosuspension prepared by the melt emulsification-high pressure homogenization method. *J. Nanomater.* **2015**, *2015*, 263. [[CrossRef](#)]
69. Wang, C.; Cui, B.; Guo, L.; Wang, A.; Zhao, X.; Wang, Y.; Sun, C.; Zeng, Z.; Zhi, H.; Chen, H. Fabrication and evaluation of lambda-cyhalothrin nanosuspension by one-step melt emulsification technique. *Nanomaterials* **2019**, *9*, 145. [[CrossRef](#)]
70. Severino, P.; Fangueiro, J.F.; Chaud, M.V.; Cordeiro, J.; Silva, A.M.; Souto, E.B. Advances in nanobiomaterials for topical administrations: New galenic and cosmetic formulations. In *Nanobiomaterials in Galenic Formulations and Cosmetics*; Elsevier: Amsterdam, The Netherlands, 2016; pp. 1–23.
71. Fábregas, A.; Miñarro, M.; García-Montoya, E.; Pérez-Lozano, P.; Carrillo, C.; Sarrate, R.; Sánchez, N.; Ticó, J.; Suñé-Negre, J. Impact of physical parameters on particle size and reaction yield when using the ionic gelation method to obtain cationic polymeric chitosan–tripolyphosphate nanoparticles. *Int. J. Pharm.* **2013**, *446*, 199–204. [[CrossRef](#)]
72. Yang, H.-C.; Hon, M.-H. The effect of the molecular weight of chitosan nanoparticles and its application on drug delivery. *Microchem. J.* **2009**, *92*, 87–91. [[CrossRef](#)]
73. Guan, H.; Chi, D.; Yu, J.; Li, X. A novel photodegradable insecticide: Preparation, characterization and properties evaluation of nano-Imidacloprid. *Pestic. Biochem. Physiol.* **2008**, *92*, 83–91. [[CrossRef](#)]
74. Qian, K.; Shi, T.; Tang, T.; Zhang, S.; Liu, X.; Cao, Y. Preparation and characterization of nano-sized calcium carbonate as controlled release pesticide carrier for validamycin against *Rhizoctonia solani*. *Microchim. Acta* **2011**, *173*, 51–57. [[CrossRef](#)]
75. Paulraj, M.G.; Ignacimuthu, S.; Gandhi, M.R.; Shajahan, A.; Ganesan, P.; Packiam, S.M.; Al-Dhabi, N.A. Comparative studies of tripolyphosphate and glutaraldehyde cross-linked chitosan-botanical pesticide nanoparticles and their agricultural applications. *Int. J. Biol. Macromol.* **2017**, *104*, 1813–1819. [[CrossRef](#)]
76. Rajkumar, V.; Gunasekaran, C.; Paul, C.A.; Dharmaraj, J. Development of encapsulated peppermint essential oil in chitosan nanoparticles: Characterization and biological efficacy against stored-grain pest control. *Pestic. Biochem. Physiol.* **2020**, *170*, 104679. [[CrossRef](#)]
77. Wang, A.; Wang, Y.; Sun, C.; Wang, C.; Cui, B.; Zhao, X.; Zeng, Z.; Yao, J.; Yang, D.; Liu, G. Fabrication, characterization, and biological activity of avermectin nano-delivery systems with different particle sizes. *Nanoscale Res. Lett.* **2018**, *13*, 2. [[CrossRef](#)] [[PubMed](#)]
78. Khandelwal, N.; Barbole, R.S.; Banerjee, S.S.; Chate, G.P.; Biradar, A.V.; Khandare, J.J.; Giri, A.P. Budding trends in integrated pest management using advanced micro-and nano-materials: Challenges and perspectives. *J. Environ. Manag.* **2016**, *184*, 157–169. [[CrossRef](#)] [[PubMed](#)]
79. Melanie, M.; Miranti, M.; Kasmara, H.; Malini, D.M.; Husodo, T.; Panatarani, C.; Joni, I.M.; Hermawan, W. Nanotechnology-based bioactive antifeedant for plant protection. *Nanomaterials* **2022**, *12*, 630. [[CrossRef](#)]
80. Amidi, M.; Romeijn, S.G.; Borchard, G.; Junginger, H.E.; Hennink, W.E.; Jiskoot, W. Preparation and characterization of protein-loaded N-trimethyl chitosan nanoparticles as nasal delivery system. *J. Control. Release* **2006**, *111*, 107–116. [[CrossRef](#)]
81. Grenha, A.; Grainger, C.I.; Dailey, L.A.; Seijo, B.; Martin, G.P.; Remuñán-López, C.; Forbes, B. Chitosan nanoparticles are compatible with respiratory epithelial cells in vitro. *Eur. J. Pharm. Sci.* **2007**, *31*, 73–84. [[CrossRef](#)]
82. Grillo, R.; Pereira, A.E.; Nishisaka, C.S.; De Lima, R.; Oehlke, K.; Greiner, R.; Fraceto, L.F. Chitosan/tripolyphosphate nanoparticles loaded with paraquat herbicide: An environmentally safer alternative for weed control. *J. Hazard. Mater.* **2014**, *278*, 163–171. [[CrossRef](#)] [[PubMed](#)]
83. Silva, M.; Concenza, D.; Grillo, R.; Melo, N.; Tonello, P.; Oliveira, L.; Cassimiro, D.; Rosa, A.; Fraceto, L. Paraquat-loaded alginate/chitosan nanoparticles: Preparation, characterization and soil sorption studies. *J. Hazard. Mater.* **2011**, *190*, 366–374. [[CrossRef](#)] [[PubMed](#)]